

## ASSESSMENT OF THE INFRARED WELDING PROCESS FOR A CARBON FABRIC REINFORCED PPS

K. Allaer\*, I. De Baere, S. Jacques, W. Van Paepegem and J. Degrieck

*Department of Materials Science and Engineering, Ghent University, Technologiepark 903, B-9052 Ghent.*

*\*Klaas.Allaer@ugent.be*

**Keywords:** Fusion bonding, Mode I DCB , Mode II ENF, Thermoplastic

### **Abstract**

*This study assesses the use of infrared welding for a carbon fabric reinforced polyphenylene sulphide. Infrared light is used in order to melt the thermoplastic matrix of the two components, after which they are joined together under pressure. Welding parameters such as power of the infrared lights, heating time, contact pressure and consolidation time are optimised. Next, a series of joints is fabricated and the interlaminar behaviour of the weld is characterised. For the mode I behaviour, the Double Cantilever Beam test (DCB) is considered, whereas for mode II crack growth, the End Notch Flexure test (ENF) is used. Results are compared to the interlaminar behaviour of the base material. It can be concluded that the infrared process proves very interesting for the material under study and that joints can be manufactured with fracture toughness values equal or higher to the base material, both for mode I and mode II, but that a slightly different failure behaviour manifests itself.*

### **1. Introduction and Principle**

As the industry starts to see the growing potential of fibre reinforced thermoplastics, it is more likely to choose this group of reinforced plastics over the fibre reinforced thermosetting polymers. However, where thermosetting polymers are in general easily bonded using adhesives, this is not always the case for thermoplastics, given their chemical inertness. As load bearing joints cannot always be avoided, there is a growing interest for welding processes or fusion bonding of thermoplastic composites. In general, these fusion bonding techniques can be categorised in three groups [1]: (i) frictional welding, including ultrasonic welding [2, 3]; (ii) electromagnetic welding, including resistance welding [4, 5] and induction welding [6, 7] and (iii) thermal welding, including infrared welding [8]. To assess the strength and reproducibility of the weld, quasi-static experiments till failure are quite often considered. Until now, there is not yet a standardised method for testing welded joints, but there are various standards and test setups available for examining the strength of adhesive bonds or the growth of delaminations [9, 10]. For evaluating the strength and the quality of the welds, the most commonly chosen experimental setups are the Lap Shear Strength test (LSS) [2, 4, 5] and the Double Cantilever Beam test (DCB) [4,5, 8]. These methods give relevant information about the quality of the weld and are also quite useful for comparative studies.

## 2. Materials and Methods

### 2.1. Composite Material

The material under study was a carbon fibre-reinforced polyphenylene sulphide (PPS), called CETEX. This material is supplied to us by Ten Cate. The fibre type is the carbon fibre T300J 3K and the weaving pattern is a 5-harness satin weave with a mass per surface unit of 286 g/m<sup>2</sup>. The 5-harness satin weave is a fabric with high strength in both directions and excellent bending properties. The carbon PPS plates were hot pressed at 10 bars and 310 °C; only one stacking sequence was used for this study, namely [(0°,90°)]<sub>4s</sub> where (0°,90°) represents one layer of fabric. The in-plane elastic properties of the individual carbon PPS lamina were determined by the dynamic modulus identification method as described in [11] are represented in Table 1.

$E_{11}$	56.0	GPa	$X_T$	734.0	MPa
$E_{22}$	57.0	GPa	$\epsilon_{11}^{ult}$	0.011	-
$\nu_{12}$	0.033	-	$Y_T$	754.0	MPa
$G_{12}$	4.175	GPa	$\epsilon_{22}^{ult}$	0.013	-
			$S_T$	110.0	MPa

**Table 1.** In-plane elastic and tensile strength properties of the individual carbon/PPS lamina.

Figure 1 shows the geometry of a fusion bonded batch of single lap shear specimen. The dimensions are chosen according to the ASTM D5868-01 ‘Standard Test Method for Lap Shear Adhesion for Fiber Reinforced Plastic Bonding’.

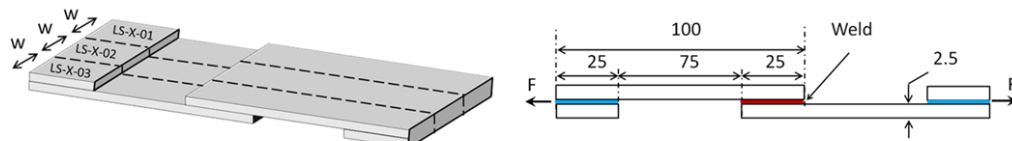
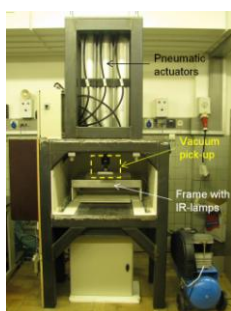


**Figure 1.** Dimensions of the used single lap shear specimen (in mm).

### 2.2. Equipment

All tensile tests were performed on an servo-hydraulic INSTRON 8801 tensile testing machine with a FastTrack 8800 digital controller and a load cell of  $\pm 100$ kN. The quasi-static tests were displacement-controlled with a displacement speed of 1 mm/min. The load  $F$  and displacement  $\delta$ , given by the FastTrack controller, were sampled on the same time basis. The in-house developed infrared welding setup, including power electronics and pneumatics, is shown in Figure 2(a). Figure 2(b) shows a detail of the infrared welding lamps, mounted in the movable frame.



(a) Total setup



(b) IR-lights within frame

**Figure 2.** The infrared welding setup.

The pneumatic actuators operate at 10 bar, yielding each a maximum force of 22.5 kN. The infrared lights use a carbon filament and generate a power of 4000 W each. A separate control system continuously monitors the temperature of the specimens, using a non-contact temperature sensor or a thermocouple and controls the power sent to the IR-set.

### 3. Experiments and Discussion

#### 3.1. The infrared welding process

Preliminary tests have shown that joints made between the standard specimens were of poor quality, since there was insufficient thermoplastic material present to form a joint [12]. As such, extra layers of PPS should be added to the weld. A first attempt was made simply by laying the layers of PPS on the bottom sample and allowing them to melt in the same melting phase as the specimens. This principle, referred to as ‘one sided welding’ worked, but yielded poor quality and poor reproducibility of the bonds, as will be shown later in this manuscript. Therefore, it was decided to add the PPS in a separate phase prior to welding, as illustrated in Figure 3(a) and (b): in a first preparation phase (Figure 3(a), referred to as phase 1), layers of PPS are placed exactly on the location where the bond is expected (1). The remaining area of the specimen is shielded with a kapton tape, so that this area would not melt. Next, the specimens are heated until the PPS has melted (2), which is determined by the temperature measurement. In the final preparation step (3) the PPS is pushed on the surface with a polished aluminium plate, using only a mild pressure, enough to ensure a flat surface. In the actual welding phase (Figure 3(b)), referred to as phase 2), the specimens are first placed according to the desired geometry (4). Next (5), the top specimen is lifted with the plunger and the vacuum setup and after the temperature sensor is attached to the bottom sample, both specimens are heated until the desired temperature and/or enough PPS has melted, after which the infrared lights are removed and the plunger applies the necessary consolidation pressure (6).

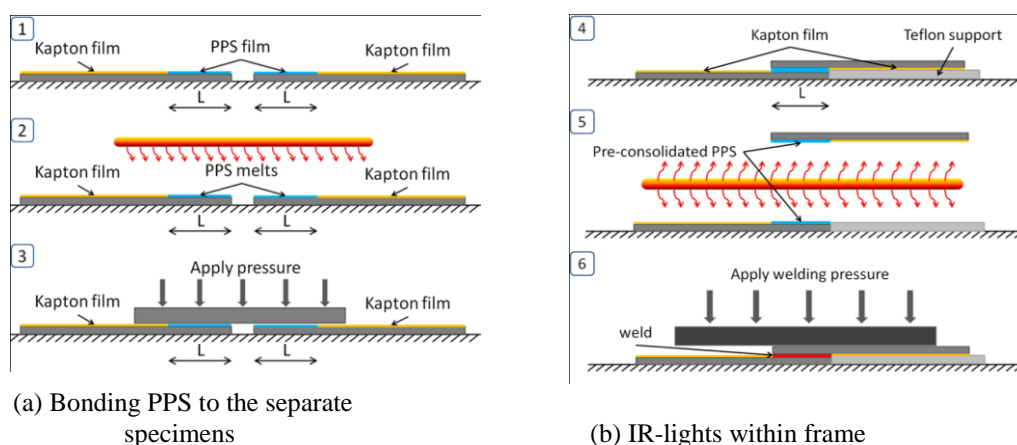


**Figure 3.** Welding procedure, illustrated for a lapshear specimen.

The paragraph above describes the process called ‘two sided welding’, since PPS is pre-consolidated on both adherends prior to welding.

#### 3.2. Lapshear experiments

As there is not yet a testing standard for fusion bonded joints, the standards regarding the testing of adhesively bonded single lap joints are considered. The geometry is

chosen according to the ASTM D5868-01 ‘Standard Test Method for Lap Shear Adhesion for Fiber Reinforced Plastic Bonding’. This means that the specimen has a geometry as illustrated in Figure 1.

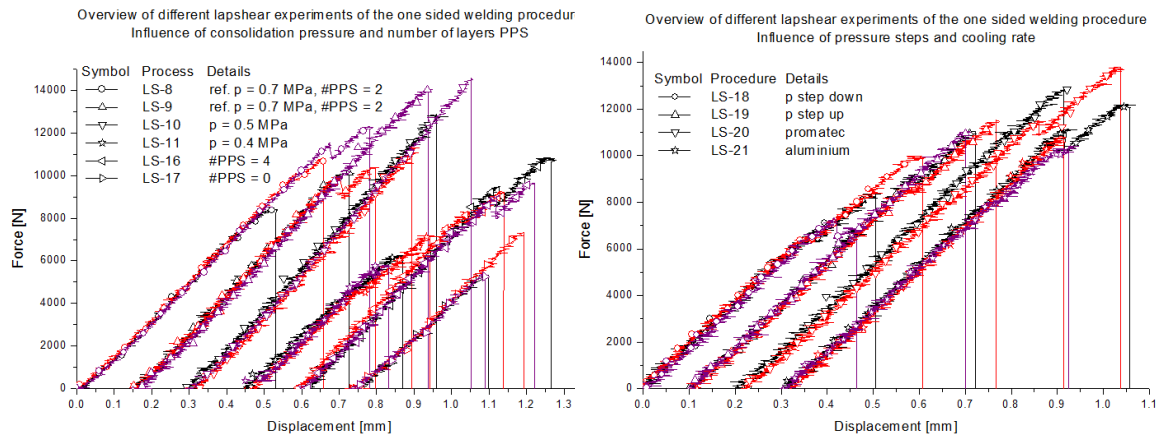
### 3.2.1. One sided Welding

Table 2 shows an overview of the used parameters for the one sided welding process. Results from the lapshear experiments are shown in Figure 4, each cycle is given an offset on the horizontal axis to improve the clarity. The consolidation time ( $t_{\text{consolidate}}$ ), was the time to reach a temperature below 80°C, so beneath the glass transition temperature of the PPS, the column ‘# PPS’ refers to the number of sheets of PPS (thickness 100  $\mu\text{m}$ ) which were added to the weld.

Welding cycle	Pressure [MPa]	# PPS [-]	$t_{\text{melt}}$ [s]	$t_{\text{consolidate}}$ [s]	Pressure [MPa]	# PPS [-]	$t_{\text{melt}}$ [s]	$t_{\text{consolidate}}$ [s]
LS-8	0.7	2	125	255	LS-19	0.3	2	142
LS-9	0.7	2	130	250		0.5		120
LS-10	0.5	2	125	248		0.7		135
LS-11	0.4	2	150	265	LS-20	0.7	2	115
LS-16	0.7	4	135	270	LS-21	0.7	2	115
LS-17	0.7	0	120	265				235
LS-18	0.7	2	150	120				
	0.5			165				
	0.3			165				

**Table 2.** Overview of the different welding parameters for the one sided welding procedure.

Cycles 8 and 9 are used as a reference, to illustrate the effect of variations in the parameters considered for the other cycles. As both have virtually the same process parameters, the reproducibility between similar welding cycles can also be assessed. As can be seen in Figure 4(a), the reproducibility for cycle 8 and 9 is fairly non-existent. For cycles 10 and 11, the pressure during consolidation was lowered. This has a positive effect for cycle 10, resulting in higher strengths, but when the pressure becomes too low, the strength also significantly decreases. Pressures between 0.5 and 0.7 MPa seemed to be optimum values regarding this effect. For cycles 16 and 17, the amount of PPS sheets placed inside the weld was varied. For LS-16, a lot more of the liquid PPS was pushed out of the weld compared to the other cycles, partially undoing the extra layers, but nevertheless, a lower strength was achieved. More layers of PPS combined with a lower pressure, to avoid the PPS push out, also resulted in lower strengths. Using no extra sheets of PPS has an even worse effect on the failure forces of the bond, as they are the lowest of all experiments discussed here. As such, two layers of PPS seem to be an optimum for this welding procedure. For cycles 18 and 19, the influence of the pressure during consolidation was examined. For LS-18, the pressure started at 0.7 MPa and was then lowered to 0.5 when the temperature in the bond reached 185°C. When reaching 135°C, the pressure was lowered to 0.3 MPa until the temperature was below 80°C. For LS-19, the opposite was chosen, the pressure was increased at the mentioned temperature levels. Apparently, stepwise lowering the pressure has a negative effect on the strength, whereas stepwise increasing the pressure has a positive effect on the strength. It should be mentioned that by the time the first pressure was applied, the temperature had already dropped to around 240 °C, depending on the cycle.



(a) Force versus displacement of the one sided welding procedure (part I). (b) Force versus displacement of the one sided welding procedure (part II).

**Figure 4.** Force versus displacement for the different parameter settings.

This, however, is an important temperature for PPS, as this is the temperature around which crystallisation occurs during cooling down. Therefore, it was attempted to reduce the cooling rate by using a Promatec buffer. Cycles 20 and 21 have exactly the same settings, only the different buffer was used, resulting in different consolidation times. However, the use of the Promatec buffer clearly has a positive influence on the strength of the bond.

### 3.2.2. Two sided welding

As the Promatec buffer and the resulting lower cooling rate clearly improved the lapshear strength for the one sided welding, the aluminium buffer is no longer considered for phase 2 of the two sided welding procedure. To shorten time, the aluminium buffer was still used for phase 1, hence the shorter consolidation times in Table 3.

Welding cycle	Pressure [MPa]	# PPS [-]	$t_{melt}$ [s]	$t_{consolidate}$ [s]	Pressure [MPa]	# PPS [-]	$t_{melt}$ [s]	$t_{consolidate}$ [s]	
LS-22-phase1	0.7	2x2	135	200	LS-24-phase1	0.7	2x1	135	225
LS-22-phase2	0.5		135	273	LS-24-phase2	0.3		120	146
LS-23-phase1	0.7	2x3	165	210		0.7			260
LS-23-phase2	0.7		130	148	LS-25-phase1	0.7	2x1	125	235
	0.5			180	LS-25-phase2	0.7		115	280

**Table 3.** Overview of the different welding parameters for the two sided welding procedure.

Figure 5 shows the results of the lapshear experiments corresponding to the settings mentioned in Table 3. Firstly, the reproducibility within one welding cycle is very high. Secondly, even between batches with different settings, which in some cases had a significant influence for the one sided welding procedure, the reproducibility is still remarkable. The last cycle, LS-25, shows that there are limits on the process window, as the strength of this cycle is lower than the others. Apparently, the combination of only two layers of PPS with a consolidation pressure of 0.7 leaves insufficient PPS in the bond to achieve a high strength. Figure 6(a) shows a lapshear experiment on one of the samples.

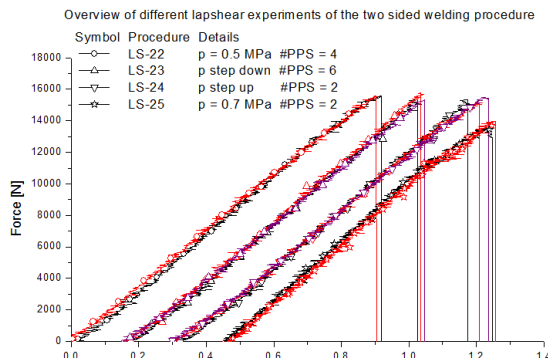


**Figure 5.** Force versus displacement for the different parameter settings during the two sided welding procedure.

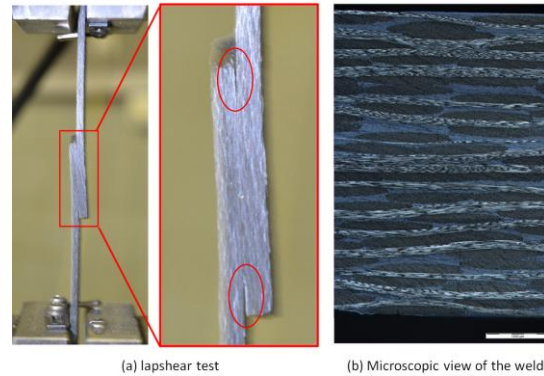


**Figure 6.** Illustration of the lapshear test and a successful bond

As such, there is a limited amount of crack growth prior to failure. Figure 6(b) shows a microscopic view of a section of a bond and no porosities could be distinguished, meaning a successful weld is achieved. This was of course verified over the entire cross section of the specimen. Finally, **Table 4** gives an overview of the strengths of the lapshear specimens for the different settings for both the one sided and two sided welding. For each cycle, both the average failure load ( $F_{\text{average}}$ ) and the difference between the maximum and the minimum failure load of the tested specimens for that run is given. For comparison purposes, also the corresponding, but not occurring ‘average shear stress’  $\tau_{13}^{\text{average}}$ , calculated as the failure load divided by the intended surface of  $625 \text{ mm}^2$  and the difference between maximum and minimum are also given in the table, both in absolute value, and relative to the average value (scatter).

Welding Cycle	$F_{\text{average}}$ [N]	$F^{\text{max}} - F^{\text{min}}$ [N]	$\tau_{13}^{\text{average}}$ [MPa]	$\tau_{13}^{\text{max}} - \tau_{13}^{\text{min}}$ [MPa]	scatter [%]
One sided welding					
LS-8	10363	3918	16.58	6.27	38
LS-9	11512	3934	18.42	6.29	34
LS-10	12922	3254	20.67	5.21	25
LS-11	6380	1383	10.21	2.21	22
LS-16	9900	1590	15.84	2.54	16
LS-17	3901	1306	6.24	2.09	33
LS-18	8416	3103	13.47	4.96	37
LS-19	11203	494	17.92	0.79	4.4
LS-20	13329	925	21.33	1.48	6.9
LS-21	11145	1796	17.83	2.87	16
Two sided welding					
LS-22	15589	29	24.94	0.05	0.2
LS-23	15485	432	24.78	0.69	2.8
LS-24	15288	289	24.46	0.46	1.9
LS-25	13747	450	22.00	0.72	3.3

**Table 4.** Overview of the achieved strengths for the considered welding parameters

Although the one sided welding sometimes yields high failure loads, the scatter on these results is very high, making this procedure unpredictable. As such, the two sided welding is preferable, as the achieved strength is not only higher, it is also combined

with very low scatter, making it more predictable. To try and determine a reason for the difference in failure strength and scatter between both welding processes, the fracture surfaces of some specimens were examined with Scanning Electron Microscopy. Figure 7 illustrates a few examples of representative images, where the main difference can clearly be distinguished. For the one sided welding process (Figure 7(a)), cavities of various sizes, such as the ones illustrated, were always present on the surface, but they were not evenly distributed over the entire surface, possibly causing the larger scatter on the results. Such cavities were never found for the two sided welding procedure, the entire fracture surfaces was similar to the images shown in (Figure 7(b)).

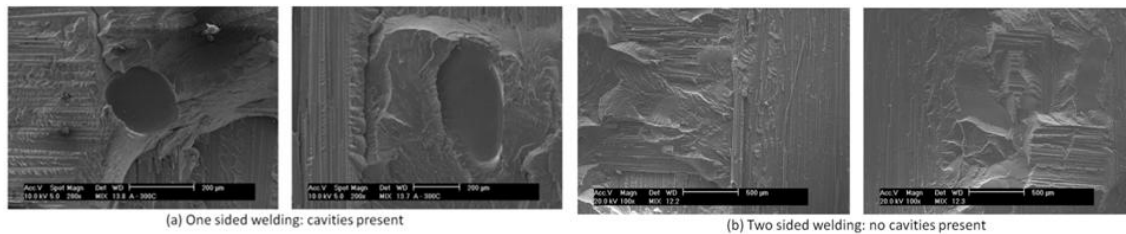


**Figure 7.** SEM observation of the fracture surfaces of both welding processes.

The question remains whether this is the highest strength achievable with the material under study. Given the very low scatter and excellent reproducibility for the two sided welding, the authors feel that the achieved strength will indeed approximate the maximum possible with the current setup, meaning without accurate control of the cooling rate during consolidation. However, the combined effects of weld pressure, temperature and time on interdiffusion and optimal crystallisation have not yet been considered, as this is not yet possible with the current setup. This, however, may have a significant influence on the bond strength, and has already been documented in literature, both under isothermal as non-isothermal conditions [13, 14, 15].

For this manuscript, all welds were manufactured within the boundary conditions of the currently used infrared welding setup, where the heating temperature, consolidation pressure and the respective time intervals can be controlled. The cooling rate during consolidation, cannot yet be controlled, it can only be influenced by use of different buffer materials, but even within this limits, high quality welds are achieved.

#### 4. Conclusions

This manuscript studied the infrared welding process for a 5-harness satin weave carbon reinforced polyphenylene sulphide. The quality and strength of the welded joints were assessed using lapshear experiments according to the ASTM D5868-01 'Standard Test Method for Lap Shear Adhesion for Fiber Reinforced Plastic Bonding'. Two types of welding procedures were assessed where the main difference lies in the way extra sheets of PPS are added to the bond. For each welding cycle, a bond was formed out of which three lapshear specimens could be cut. It was found that although high failure loads were possible, the one sided welding yielded very irreproducible results, not only between separate welding cycles with the same settings, but also between the three specimens coming from one cycle, which of course cannot be allowed. The two sided welding showed very reproducible results, both within one welding cycle as when comparing different welding cycles. Furthermore, there seems to be little influence, within certain boundaries, of the amount of PPS added and the consolidation pressure, yielding a bigger process window. The latter is of course interesting if this technique is to be implemented in real life production.

## Acknowledgements

The authors are highly indebted to the Fund of Scientific Research – Flanders (F.W.O.) for sponsoring this research and to Ten Cate Advanced Composites for supplying the material. Also special thanks to L. Vanden Broecke for his contributions to this work.

## References

- [1] Yousefpour A, Hojjati M, Immarigeon JP, Fusion bonding/welding of thermoplastic composites. JOURNAL OF THERMOPLASTIC COMPOSITE MATERIALS 17 (4): 303-341 JUL 2004.
- [2] Jandali G, Mallick PK. Vibration welding of a unidirectional continuous glass fiber reinforced polypropylene GMT. COMPOSITES PART A-APPLIED SCIENCE AND MANUFACTURING 36 (12): 1687-1693 2005.
- [3] Gutnik VG, Gorbach NV, Dashkov AV, Some characteristics of ultrasonic welding of polymers. FIBRE CHEMISTRY 34 (6): 426-432 NOV-DEC 2002.
- [4] Hou M, Yang MB, Beehag A, Mai YW, Ye L. Resistance welding of carbon fibre reinforced thermoplastic composite using alternative heating. COMPOSITE STRUCTURES 47 (1-4): 667-672 DEC 1999.
- [5] Ageorges C, Ye L, Hou M. Experimental investigation of the resistance welding for thermoplastic-matrix composites. Part I: heating element and heat transfer. COMPOSITES SCIENCE AND TECHNOLOGY 60 (7): 1027-1039 2000.
- [6] Kagan VA, Nichols RJ. Benefits of induction welding of reinforced thermoplastics in high performance applications. JOURNAL OF REINFORCED PLASTICS AND COMPOSITES 24 (13): 1345-1352 2005.
- [7] W. Suwanwatana, S. Yarlagadda and J.W. Gillespie, Jr. Hysteresis heating based induction bonding of thermoplastic composites . COMPOSITES SCIENCE AND TECHNOLOGY 66 (11-12): 1713-1723 SEP 2006.
- [8] Lamethe JF, Beauchene P, Leger L. Polymer dynamics applied to PEEK matrix composite welding. AEROSPACE SCIENCE AND TECHNOLOGY 9 (3): 233-240 APR 2005.
- [9] Szekrenyes, Andras. Improved analysis of unidirectional composite delamination specimens. MECHANICS OF MATERIALS 39 (10): 953-974 OCT 2007.
- [10] Mathews, Mary J. and Swanson, Stephen R. Characterization of the interlaminar fracture toughness of a laminated carbon/epoxy composite. COMPOSITES SCIENCE AND TECHNOLOGY 67 (7-8): 1489-1498 JUN 2007.
- [11] De Baere I, Van Paepegem W., Degrieck J., Sol H., Van Hemelrijck D. and Petreli A., Comparison of different identification techniques for measurement of quasi-zero Poisson's ratio of fabric reinforced laminates. Composites A 38 (9) pp. 2047-2054. (2007)
- [12] De Baere I, Van Paepegem W. and Degrieck J. Feasibility study of fusion bonding for carbon fabric reinforced polyphenylene sulphide by hot-tool welding.  
ACCEPTED for Journal of Thermoplastic Composites
- [13] Bastien, L. J. and J. W. Gillespie Jr., "A Nonisothermal Healing Model for Strength and Toughness of Fusion Bonded Joints of Amorphous Thermoplastics," Polymer Engineering and Science, Vol. 31, No. 24, pp. 1720–1730, December 1991
- [14] Tierney, J., J. W. Gillespie, Jr., "Modeling of In-Situ Strength Development for the Thermoplastic Composite Tow Placement Process," Journal of Composite Materials, 40 (16) pp. 1487-1506, 2006.
- [15] Tierney, J. and J. W. Gillespie, Jr. "Crystallization Kinetics Behavior of PEEK-based Composites Exposed to High Heating and Cooling Rates," Composites Part A: Applied Science and Manufacturing, Vol. 35, pp. 547-558, 2004.